

УДК 619.71

**A. Prach**

## **A LATERAL AUTOPILOT FOR A TACTICAL UAV**

### **Introduction**

Multiple control strategies and techniques are used for designing controllers for UAVs. PID is the control algorithm most often used in process control. Thus [1] illustrates flight control system that uses PID controller gain scheduling algorithm based on the airspeed. In [2] PID uses model inversion in a PID controller algorithm, which is used for autonomous landing for the UAV. A key aspect in the efficiency of control algorithm is its ability to accommodate changing dynamics and payload configurations automatically. Many factors have an effect upon the performance of the controller, such as parametric uncertainty (changing mass, and aerodynamic characteristics), unmodeled dynamics, actuator magnitude and rate saturation, sensor noise, and atmospheric disturbances (turbulence, gust), and assumptions made during control design itself. Parametric uncertainty limits the operational envelope of the vehicle to where control designs are valid, whereas unmodeled dynamics and saturation

can severely limit the achievable bandwidth of the system. The effect of

uncertainty and unmodeled dynamics have been successfully handled using robust control techniques [3], [4].

### **Problem Formulation**

In this paper lateral autopilots for a TUAV are designed by means of classical control theory (PID controller) and robust control theory ( $H_\infty$  controller). Implemented control algorithms must guarantee satisfactory input tracking performance in the face of significant uncertainties and disturbances acting upon the system. The uncertainties are assumed to be bounded in size by some constant, or by some well-defined functions.

### **Mathematical Model of the UAV, EOM Linearization and Stability Analysis**

A tactical UAV (TUAV) is used as a platform for this work. 6-DoF nonlinear model of the TUAV, which consists of several blocks, which represent

vehicle's aerodynamics, environment, forces and moments computation block, etc., is developed in MATLAB/Simulink.

Linear model of the lateral motion of the UAV is obtained by linearization of nonlinear equations of motion (EOM). Linearization is performed around a certain trim point: velocity in x-direction in body axis  $u_0 = 36 \text{ m/s}$ , velocity in z-direction in body axis  $w_0 = 1.81 \text{ m/s}$ , pitch angle  $\theta = 4.4 \text{ deg}$ ,  $Thrust = 100 \text{ H}$ .

States, which correspond to the lateral dynamics of an aircraft, are: side velocity in body axis ( $v$ ), roll rate ( $p$ ), yaw rate ( $r$ ) and roll angle ( $\phi$ ). To control the lateral motion ailerons and rudder are used. State and control matrices, which describe lateral motion of an aircraft are as given below:

$$A_{lat} = \begin{bmatrix} -0.173 & 1.78 & -35.79 & 9.751 \\ -0.54 & -5.764 & 0.7258 & 0 \\ 0.2023 & -0.7669 & -0.6072 & 0 \\ 0 & 1.0 & 0.07705 & 0 \end{bmatrix}, \quad B_{lat} = \begin{bmatrix} 0 & 1.834 \\ 52.09 & 19.36 \\ 3.861 & -3.636 \\ 0 & 0 \end{bmatrix}$$

The lateral motion of aircraft is described by three dynamic modes: roll mode, dutch-roll mode and spiral mode, characteristics of which are given in tables 1 and 2.

**Table 1.**

**Dutch-roll Mode Characteristics**

Mode Name	Root Location	Natural Frequency $\omega_n$ (rad/s)	Period (s)	Damping ratio $\xi$	Time to Half Amplitude $t_{half}$ (s)
Dutch-roll	$-0.2441 \pm 3.2075i$	3.216	1.953	0.076	2.826

**Table 2.**

**Roll and Spiral Mode Characteristics**

Mode Name	Root Location	Time Constant (s)	Time to Half Amplitude $t_{half}$ (s)
Roll	-6.0467	0.165	0.114
Spiral	-0.0092	108.695	75.0

### Control System Requirements

Requirements to the control system are defined with respect to the system's tracking performance in terms of its response to a unit step input and are the following: overshoot  $< 10\%$ ; settling time  $< 3 \text{ sec}$ ; rise time  $< 1 \text{ sec}$ ; steady state error  $< 2\%$ .

## Design of a Classical Controller

PID controller, which is referred to as a classical controller, is used for a lateral autopilot of the TUAV. Fig. 1 illustrates a basic configuration of a feedback control system.

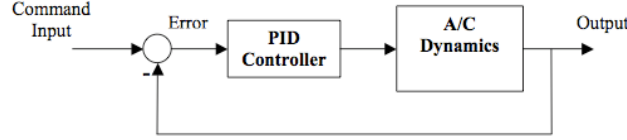


Fig. 1. Basic Control System Configuration

Dynamics of the UAV is represented by the linearized lateral dynamic: transfer function from ailerons deflection to roll angle of the airplane:

$$W_{\varphi/\delta a} = \frac{52.4s^3 + 42.1s^2 + 458.3s}{s^4 + 6.544s^3 + 13.36s^2 + 62.69s + 0.5783}$$

and model of the actuator, which is assumed to be a first order servo. The transfer function of a PID controller is  $G_c = -K_p[1 + 1/(sT_i) + sT_d]$ . Choice of values of the controller's parameters (proportional gain, integral time and derivative time) can be performed by different techniques. For purposes of this work, PID tuning methods described in [5] are used. However, these rules, which are based on step response of the plant, provide a response with 10%-60% maximum overshoot. For this reason, an experimental tuning is used to tune controller's gains such that response of the closed-loop system would be satisfactory for the nominal plant, and for the perturbed plant and with a sensor noise presence as well.

The following values of controller parameters are chosen:  $K_p=2.5$ ,  $T_i=1.66$ ,  $T_d=0.12$ . Transfer function of the PID controller:  $G_c = 2.5 \left( 1 + \frac{1}{1.66s} + 0.12s \right) = \frac{0.3s^2 + 2.5s + 1.5}{s}$ . Response of the

closed-loop system, which includes nonlinear dynamics of the TUAV, to a unit step input in terms of roll angle and ailerons position is shown in fig. 2, 3. Simulation results show that tracking performance of the control system satisfies the requirements; however, controller requires too many efforts from actuator, especially in terms of ailerons' rate, that might cause saturation of the actuators.

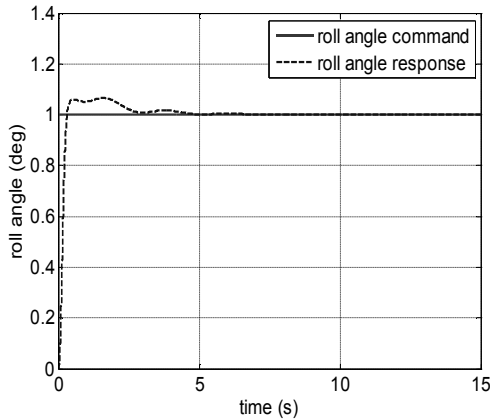


Fig. 2. System Response to a Unit Step Input Roll Angle

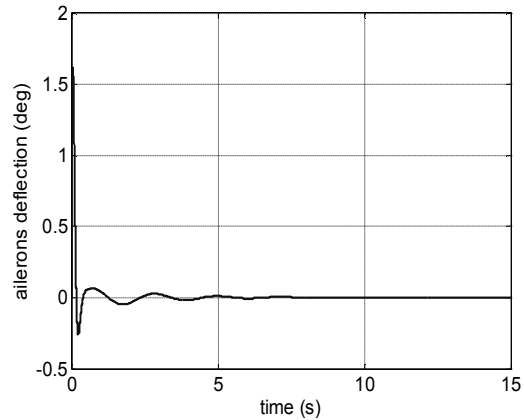


Fig. 3. Ailerons Deflection for a Unit Step Input

### $H_\infty$ Controller Design

Controllers designed by robust techniques involve model uncertainty in their algorithms. [6], [7] and [8] explain principles of modeling of uncertainties and give the concept of the  $H_\infty$  norm and  $\mu$ -synthesis theory. Different perspectives and methods of  $H_\infty$  design technique are given in [9], [10].

General framework used for robust design is illustrated in fig.4 in which  $P$  represents a generalized plant, which is derived from the nominal plant but includes weighting functions and is also assumed Finite Dimensional Linear Time Invariant system;  $K$  represents a controller;  $w$  is an external input that includes the reference signal, disturbances, and noise;  $u$  is control input;  $y$  represents measured variables, and  $z$  represents the error signals. State space models of  $P$  and  $K$  are available and that their realizations are assumed stabilizable and detectable. Defining the transfer function from external input to errors as  $T_{zw}$ , statement for optimal  $H_\infty$  control problem is the following: “find all the admissible controllers  $K(s)$  such that  $\|T_{zw}\|_\infty$  is minimized”.

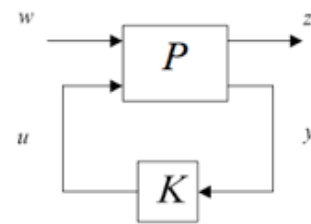


Fig. 4. General Framework

In this work design of the lateral  $H_\infty$  controller for the UAV is performed using MATLAB Robust Control Toolbox, which enables to compute a stabilizing  $H_\infty$  controller for a given plant. Consider the the block diagram of a closed-loop system as it is shown in Fig.5, in which block  $G$  represents the plant to be controlled and  $K$  represents the robust controller. Weight function  $W_m$  that represents multiplicative uncertainty, the main source of which is

change of the UAV's aerodynamic parameters. Weight function  $W_p$  characterizes controller's performance and represents the output error, it is chosen as a low-pass filter. Weighting function  $W_n$  represents effect of the sensor noise on the system's output, assuming 0.1% noise at low frequencies and 1% noise at high frequencies  $W_n$  is chosen as a high pass filter.

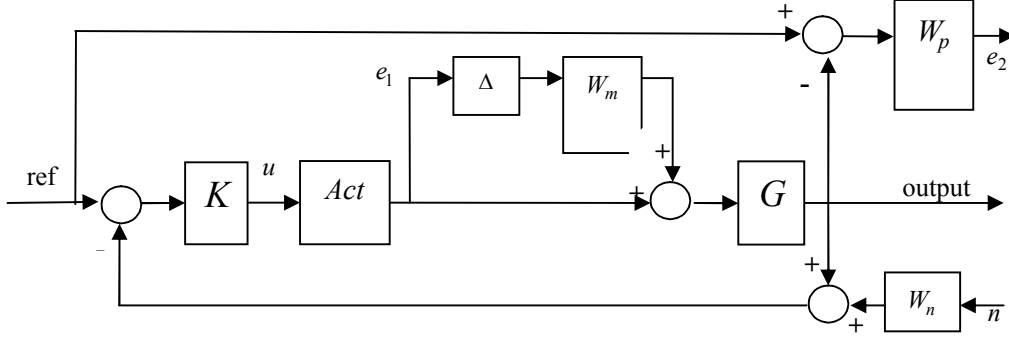


Fig. 5. Block Diagram of Closed-loop System

State space model of the  $H_\infty$  controller, which has 1 output, 1 input, and 8 states in terms of state space matrices is given below.

$$A = \begin{bmatrix} -6.544 & -3.281 & -3.906 & 0.3728 & 120 & 9.6 & -8.474 \cdot 10^{-6} & -0.8129 \\ 4 & -0.04117 & -0.00827 & -0.3601 & 0 & 0 & 1.289 \cdot 10^{-5} & 0.5658 \\ 0 & 3.826 & -0.03485 & -1.518 & 0 & 0 & -2.505 \cdot 10^{-5} & 2.384 \\ 0 & -0.05895 & 0.2382 & -0.5156 & 0 & 0 & -5.297 \cdot 10^{-5} & 0.8099 \\ -5.934 \cdot 10^5 & -1.7 \cdot 10^6 & -5.89 \cdot 10^5 & -1.375 \cdot 10^6 & -3.237 \cdot 10^4 & -3.9431 \cdot 10^5 & 3.172 \cdot 10^6 & -1.28 \cdot 10^{-10} \\ 0 & -0.01859 & -0.003734 & -0.1626 & 0 & -7 & -1.719 \cdot 10^{-6} & -0.2554 \\ 0 & -0.008123 & -0.001632 & -0.07105 & 0 & 0 & -0.05487 & -22.39 \\ 0 & -0.3573 & -0.7178 & -3.125 & 0 & 0 & 0.00293 & -995.1 \end{bmatrix},$$

$$B = [-0.005019 \quad -0.003493 \quad -0.01472 \quad -0.005001 \quad 0 \quad -0.001577 \quad 0.1382 \quad -0.03032]^T,$$

$$C = 10^6 \cdot [-2.136 \quad -6.12 \quad -2.12 \quad -49.48 \quad -0.1164 \quad -1.419 \quad 11.42 \quad -4.608 \cdot 10^{-4}],$$

$$D = 0.$$

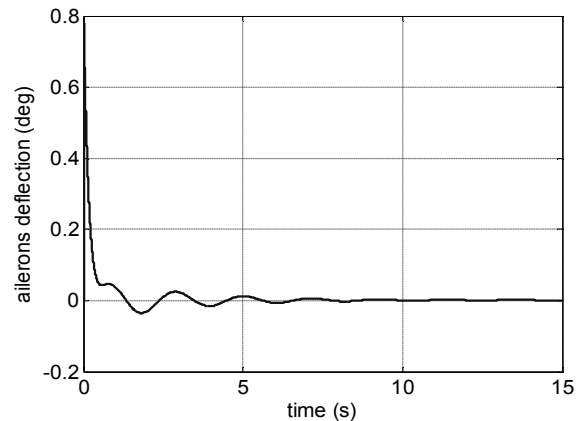
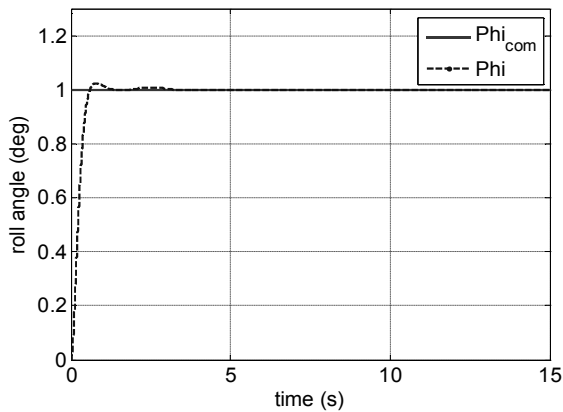


Fig. 6. Step Input Response of the Nominal Plant: Roll Angle

Performance of the controller is checked by nonlinear simulation and illustrated in fig. 6, 7 as a response of the closed-loop system to a unit step roll angle input. The results show that for a unit step input designed  $H_\infty$  controller requires very high actuator's rate at the initial input time, which can become a reason to saturation of the control surfaces.

### Robust Performance Analysis

Presence of disturbances acting on the system (wind, gusts, sensor noise) results in tracking and regulation errors. Under perturbation, performance of the closed-loop system will degrade to the point of unacceptability. Robust performance test shows the worst-case level of performance degradation associated with a given level of perturbations [9].

In this paper analysis of the robust performance of the  $H_\infty$  controller is performed by MATLAB Robust Control Toolbox [11]. "robustperf" command is used to compute the Robust Performance Margin, which is reciprocal of the input/output gain ( $H_\infty$  norm). The performance of a nominally-stable uncertain system will generally degrade (increasing gain) for specific values of its uncertain elements. Robust Performance Margin is one measure of the level of degradation brought on by the modeled uncertainty. Applying the "robustperf" command for closed-loop system the following results are obtained: upper and lower bounds on performance margin coincide and are equal to 0.9974, frequency at which the minimum robust performance margin occurs (critical frequency) 0.5460. The input/output gain remains less than 1.0026.

Fig. 8 illustrates the  $\mu$ -plot, the peak value of which is the reciprocal of the performance margin, and the frequency at which the peak occurs is the critical frequency.

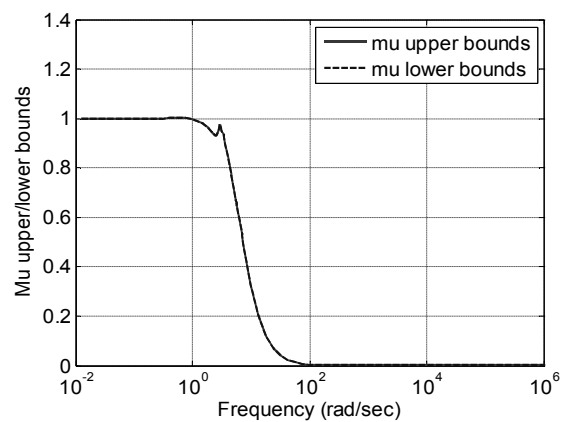


Fig. 8.  $\mu$  Plot

### Performance of the Closed-Loop System with a Command Filter

Command filters, or so-called shaping filters, are used for smoothing the input command in order to improve a system's step response by removing high frequency components from a command input, therefore reducing the overshoot of the response.

Implementation of a command filter in the closed-loop system does not affect its stability. [2] shows usage of a second order command filter, which is employed to the autoland control system for a tactical UAV. In [12] a pre-filter is implemented in order to eliminate the effect of the zero of a closed-loop transfer function on the step response. [13] introduces a time varying bandwidth command shaping filter for improving the tracking transient performance by limiting the actuator deflection rate to achievable value.

Simulations performed for PID and robust controllers for a unit step input show that both controllers require very high rate of actuators at the initial input moment. Instead of changing controllers' parameters to improve the response, command input is used to shape the input command. Responses of control systems to the filtered command input are shown in fig. 9-11.

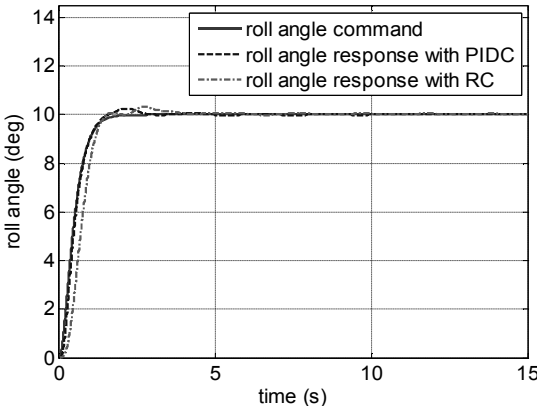


Fig. 9. Roll Angle

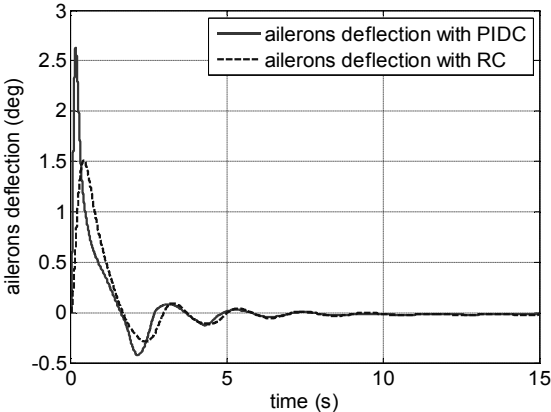


Fig. 10. Ailerons Position

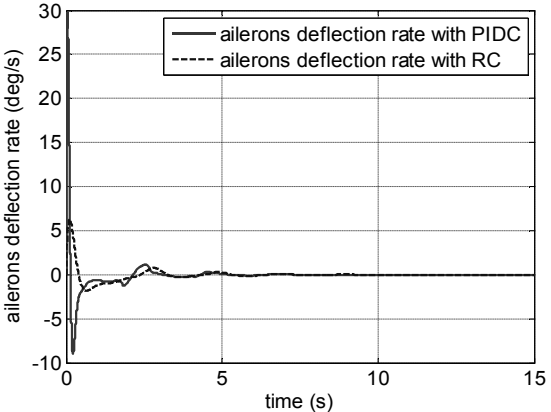


Fig. 11. Ailerons Rate

**Performance Issues for Uncertain Plant**

It has been mentioned above, it is assumed that the main source of uncertainties is in variation in aerodynamic derivatives. The most important aerodynamic derivatives that effect lateral stability of the vehicle are airplane

are effective dihedral  $C_{l\beta}$ , and roll-damping  $C_{lp}$ . In this work it is considered 5% of uncertainty with respect to the nominal value of the parameters. Simulations are performed through the nonlinear environment and its results are illustrated in fig. 12, 13.

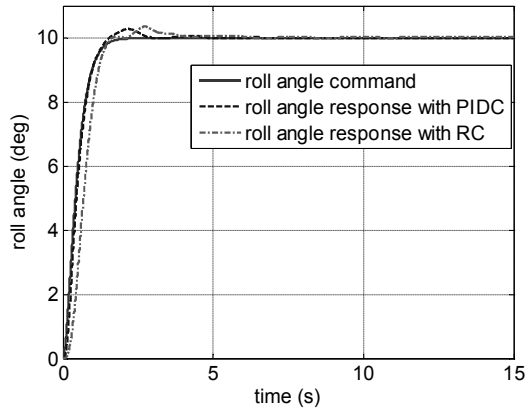


Fig.12 Roll Angle Response of Uncertain Model

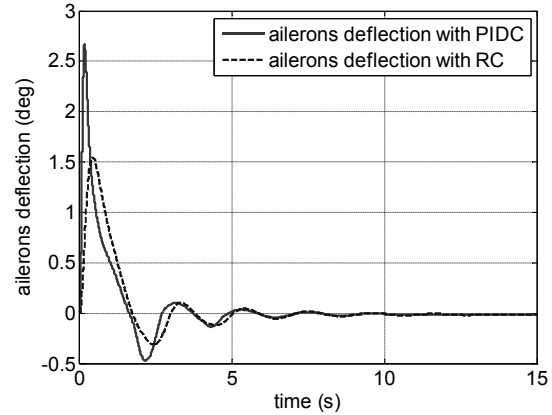


Fig.13 Ailerons Position of Uncertain Model

Simulation results illustrate, that both PID and robust controllers perform satisfactory at tracking the input signal. Such results are expected from the robust controller, which takes into account model uncertainties in design algorithm. However, it is seen that the PID controller is also able to handle with system uncertainties.

### Performance of PID and Robust Controllers with a Sensor Noise Presence

Assuming the presence of the sensor noise with a frequency of 100 Hz and standard deviation of 0.5% of the output nominal value simulations are performed for the nominal plant and the results are given in fig. 13-15 which show that both PID and robust controllers perform good in tracking the input command. However, ailerons deflection and their rate show higher sensitiveness of the PID controller to the sensor noise presence. These results are expected because noise rejection and minimization of actuator's efforts performs systematically by the  $H_\infty$  algorithm. Efficient way to decrease sensitivity of the PID controller to the noise is decreasing the derivative time  $T_d$ . However, this effects the response of the system by increasing overshoot and settling time.



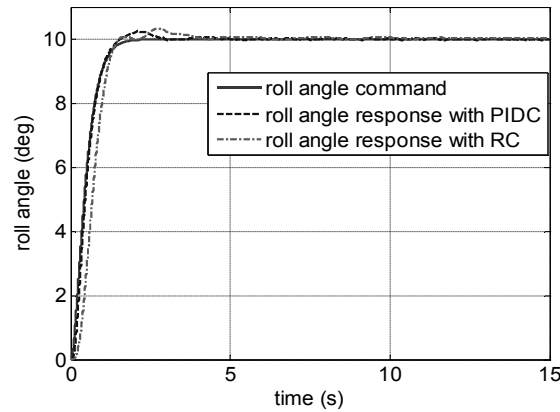


Fig.13 Roll Angle Response

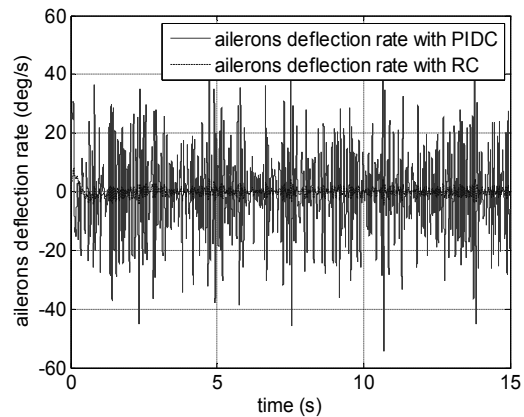
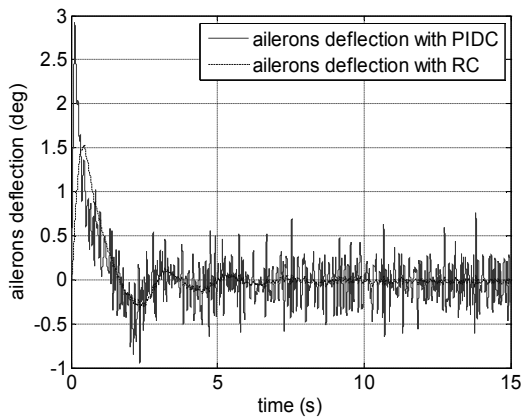


Fig. 14. Ailerons Deflection Response      Fig. 15. Ailerons Deflection Rate Response

### Conclusions

The efficiency of the PID and the  $H_\infty$  controllers designed for the TUAV is compared by multiple simulations for different cases. All requirements with respect to tracking performance are satisfied for the nominal as well as for the perturbed models. It is obvious that PID controller algorithm, which is very simple, does not take into account the uncertainties and sensor noise. Improving the noise rejection properties might have a negative effect upon the tracking performance; therefore a trade-off decision should be made with respect to system's performance and its noise rejection capabilities. Designed  $H_\infty$  controller enables to guarantee the robust performance of the closed-loop system under the model uncertainties and sensor noise presence. Therefore, if the noise rejection requirements are not of the major importance for the control system, PID algorithm is sufficient for the control purposes. If a high noise suppression is required, then a robust controller must be used.

## References

1. Fu Xu, Zhou Zhaoying, Xiong Wei, “*MEMS-Based Low-Cost Flight Control System for Small UAVs*”, Tsinghua Science and Technology, vol.13, №5, 2008.
2. V.Kargin, I.Yavrucuk, “*Autolanding Strategies for a Fixed wing UAV Under adverse Atmospheric Conditions*”, American Institute of Aeronautics and Astronautics, Guidance, Navigation and Control Conference, Honolulu, HI, USA, August 2008.
3. M. Sadraey, R. Colgren, “*Robust Nonlinear Controller Design for a Complete UAV Mission*”, AIAA Guidance, Navigation, and Control Conference and Exhibit, Keystone, Colorado, Aug. 21-24, 2006.
4. Gadewadikar, J.Lewis, F. Subbarao, K. Chen, B.M., “*Attitude Control System Design for Unmanned Aerial Vehicles using H-Infinity and Loop-shaping Methods*”, Control and Automation, 2007.
5. Ogata, Katsuhiko, “*Modern Control Engineering*”, Prentice Hall, 2002.
6. Cheng-Ching Yu, “*Autotuning of PID Controllers: A Relay Feedback Approach*”, Springer, 2006.
7. Safanov, M.G., “*Stability and Robustness of Multivariable Feedback Systems*”, M.I.T. Press, Cambridge, 1980.
8. Grimble, M.J. and Johnson, M.A., “*Optimal Control and Stochastic Estimation: Theory and Application*”, Vols 1 and 2, John Wiley & Sons, Chichester, UK, 1988.
9. K. Zhou, J.C. Doyle, “*Essentials of Robust Control*”, Prentice Hall, 1999.
10. K. Zhou, J.C. Doyle, K. Glover, “*Robust and Optimal Control*”, Prentice Hall, 1996.
11. “*Robust Control Toolbox for Use with MATLAB*”, User’s Guide, The MathWorks, Inc., 2001.
12. Richard C. Dorf, Robert H. Bishop, “*Modern Control System*”, Pearson Prentice Hall, 2005.
13. Mickle, M. C ., Zhu, J. J., “*Simulation Results for Missile Autopilot Design Based on Extended Mean Assignment*”, System Theory, Proceedings of the Twenty-Eight Southern Symposium, 1996.